CellPress

Cell Metabolism
Article

The Lysosomal v-ATPase-Ragulator Complex Is a Common Activator for AMPK and mTORC1, Acting as a Switch between Catabolism and Anabolism

Chen-Song Zhang,[1,5] Bin Jiang,[1,5] Mengqi Li,[1,5] Mingjiang Zhu,[2] Yongying Peng,[1] Ya-Lin Zhang,[1] Yu-Qing Wu,[1] Terytty Yang Li,[1] Yu Liang,[1] Zailian Lu,[1] Guili Lian,[1] Qing Liu,[1] Huiling Guo,[3] Zhenyu Yin,[3] Zhiyun Ye,[1] Jiahuai Han,[1] Jia-Wei Wu,[4] Huiyong Yin,[2] Shu-Yong Lin,[1] and Sheng-Cai Lin[1,*]

[1]State Key Laboratory for Cellular Stress Biology, School of Life Sciences, Xiamen University, Fujian 361102, China
[2]Key Laboratory of Food Safety Research, Institute for Nutritional Sciences (INS), Shanghai Institutes for Biological Sciences (SIBS), Chinese Academy of Sciences (CAS), Shanghai 200031, China
[3]Department of Hepatobiliary Surgery, Zhongshan Hospital, Xiamen University, Xiamen, Fujian 361004, China
[4]School of Life Sciences, Tsinghua University, Beijing 100101, China
[5]Co-first author
*Correspondence: linsc@xmu.edu.cn
http://dx.doi.org/10.1016/j.cmet.2014.06.014

SUMMARY

AMPK and mTOR play principal roles in governing metabolic programs; however, mechanisms underlying the coordination of the two inversely regulated kinases remain unclear. In this study we found, most surprisingly, that the late endosomal/lysosomal protein complex v-ATPase-Ragulator, essential for activation of mTORC1, is also required for AMPK activation. We also uncovered that AMPK is a residential protein of late endosome/lysosome. Under glucose starvation, the v-ATPase-Ragulator complex is accessible to AXIN/LKB1 for AMPK activation. Concurrently, the guanine nucleotide exchange factor (GEF) activity of Ragulator toward RAG is inhibited by AXIN, causing dissociation from endosome and inactivation of mTORC1. We have thus revealed that the v-ATPase-Ragulator complex is also an initiating sensor for energy stress and meanwhile serves as an endosomal docking site for LKB1-mediated AMPK activation by forming the v-ATPase-Ragulator-AXIN/LKB1-AMPK complex, thereby providing a switch between catabolism and anabolism. Our current study also emphasizes a general role of late endosome/lysosome in controlling metabolic programs.

INTRODUCTION

AMPK (AMP-activated protein kinase) is a principal sensor for energy stresses, playing crucial roles in adaptive responses to falling energy levels (Hardie et al., 2012; Steinberg and Kemp, 2009). AMPK is a heterotrimeric protein, comprised of a catalytic α subunit, a β subunit, and a γ subunit. The γ subunit is capable of binding to the adenosyl nucleotides, i.e., ATP, ADP, and AMP. When bound to ATP, the AMPK activity is inhibited. During energy stress, cellular levels of AMP are increased, leading to AMPK activation as a result of allosteric changes (Carling et al., 2012; Gowans et al., 2013; Hardie et al., 2012; Kemp, 2004; Moore et al., 1991; Xiao et al., 2007). AMP binding also promotes the upstream kinase LKB1 (liver kinase B1), in complex with STRAD and MO25, to directly phosphorylate the T172 residue in the α subunit of AMPK (Hawley et al., 2003; Oakhill et al., 2010; Sakamoto et al., 2005; Shaw et al., 2004, 2005; Woods et al., 2003), leading to its activation to a much greater extent (Chen et al., 2009; Shackelford and Shaw, 2009). AMP/ADP binding to AMPK also inhibits dephosphorylation of p-T172 of AMPK (Davies et al., 1995; Oakhill et al., 2011). Once activated, AMPK increases cellular catabolic activities to generate more ATP and meanwhile reduces energy consumption by switching off anabolic pathways (Hardie et al., 2012). We have recently reported that glucose starvation or exogenous AMP increases the affinity of myristoylated AMPK for the scaffold protein AXIN that simultaneously binds to LKB1, leading to the complex formation of AXIN/LKB1-AMPK and subsequent phosphorylation and activation of AMPK. Importantly, depletion of AXIN in the mouse liver causes severe defects in AMPK signaling (Zhang et al., 2013).

In general, while AMPK senses intracellular energy status, mTORC1 (mechanistic target of rapamycin complex 1) is activated when nutrients and growth factors are abundant (Laplante and Sabatini, 2012). Growth factors trigger activation of a series of upstream kinases, which converge to directly phosphorylate TSC1-TSC2-TBC1D7 complex, a heterotrimeric GTPase-activating protein (GAP) for the small GTPase RHEB1, and the phosphorylated GAP complex dissociates from RHEB1, rendering it GTP-bound (Dibble and Manning, 2013; Menon et al., 2014). The GTP-bound RHEB1 is located on the late endosome/lysosome surface where it binds to and activates mTORC1 (Inoki et al., 2002; Ma et al., 2005; Manning et al., 2002; Potter et al., 2002; Roux et al., 2004). In parallel, amino acids stimulate mTORC1 through modulating endosomal translocation of the mTORC1, which is directly mediated by the v-ATPase-Ragulator-RAG complex (Kim et al., 2008; Sancak et al., 2008, 2010). The Rag (Ras-related GTP binding) proteins are a class of small GTPases distinct from RHEB1, which is comprised of four members named Rag A through Rag D. The GTP-binding form of Rag A/Rag B causes translocation of mTORC1 to endosome

surfaces. Ragulator, consisting of LAMTOR1 through LAMTOR5 (late endosomal/lysosomal adaptor, MAPK and mTOR activator 1–5), is a critical pentamer complex that not only anchors RAG proteins to the endosome but also functions as their GEF (guanine nucleotide exchange factor) (Bar-Peled et al., 2012; Sancak et al., 2010). The GEF activity of Ragulator is specific to RAGA/RAGB (Bar-Peled et al., 2012). V-ATPase (vacuolar H^+-ATPase) senses high nutrient and energy levels and stimulates the GEF activity of Ragulator, which catalyzes the conversion of the GDP-bound form to the GTP-bound form of RAGA/RAGB, thereby increasing the affinity of RAGs for mTORC1 (Bar-Peled et al., 2012; Efeyan et al., 2013; Zoncu et al., 2011). As a result, mTORC1 is brought to the endosomal surface, where it becomes activated after interacting with its activator protein RHEB1 (Bai et al., 2007). Termination of mTORC1 signaling is executed by GATOR1, which functions as the GAP of RAGA/RAGB; without GATOR1, mTORC1 is constitutively active and localized on the endosomal surface (Bar-Peled et al., 2013; Panchaud et al., 2013). Opposite to AMPK, activated mTORC1 shifts the metabolic program of the cell from catabolic metabolism to anabolic metabolism by upscaling the synthesis of building blocks for cell proliferation, including proteins, lipids, and nucleotides (Laplante and Sabatini, 2012). It is thus clear that cellular homeostasis of metabolism and growth is exquisitely controlled by the coordination of AMPK and mTORC1. It was shown that activated AMPK inhibited mTORC1 by activating TSC2 (tuberous sclerosis 2) (Inoki et al., 2006) or by directly phosphorylating and subsequently inhibiting RAPTOR (regulatory-associated protein of mTOR, complex 1) (Gwinn et al., 2008). However, reports have also shown that mTORC1 can be inhibited in a TSC2- or AMPK-independent manner under energy stress (Kalender et al., 2010). Thus, how the coordination between AMPK and mTORC1 is regulated in controlling metabolic programs in response to different energy/nutrient states remains an outstanding question.

RESULTS

LAMTOR1 Is an AXIN Interactor that Is Required for AMPK Activation upon Energy Stress

To fully understand the molecular networks of the versatile scaffold protein AXIN, we performed rounds of yeast two-hybrid screen and identified LAMTOR1 (also known as P18) as a potential new AXIN-interacting protein (Figure S1A). We verified the interaction in mammalian cells by ectopically expressing AXIN and LAMTOR1 (Figure S1B). In addition, AXIN was readily coprecipitated with endogenous LAMTOR1, but not by the control IgG; the coprecipitated AXIN was decreased in *AXIN* knockdown MEFs and disappeared in *AXIN*$^{-/-}$ MEFs compared to the wild-type MEFs, indicating that the LAMTOR1-AXIN coimmunoprecipitation (co-IP) is specific (Figures 1A and S1C). As an additional control, LAMP2 (lysosome-associated membrane protein 2), another lysosomal residential protein, did not interact with Ragulator (Bar-Peled et al., 2012) or AXIN (Figure 1B), further assuring that the AXIN-LAMTOR1 interaction is specific. Since LAMTOR1 deficiency results in embryonic lethality (Nada et al., 2009), we generated *LAMTOR1*-floxed mice and crossed the mice with *albumin*-Cre mice to create liver-specific knockout mice (*LAMTOR1*^{LKO}) (Figures S1D–S1G), particularly given that in the liver AXIN is a master regulator of energy homeostasis (Zhang et al., 2013). We first assessed whether the deficiency of LAMTOR1 would have an effect on AMPK activation similar to that of AXIN, by determining phosphorylation levels of AMPKα at T172 in the liver homogenates. Induction of p-T172 by starvation was virtually abolished in the liver of *LAMTOR1*^{LKO} mice, but not in the muscle of the same mice (Figures 1C and S1J). However, it is formally possible that *LAMTOR1*^{LKO} mice might have altered activity of gluconeogenesis and have different kinetics of changes in blood glucose levels during starvation. We therefore measured blood glucose levels of *LAMTOR1*^{LKO} mice and wild-type mice and found that the blood glucose levels in both wild-type and mutant mice significantly declined after starvation, although the mutant mice indeed showed modestly higher blood glucose levels (Figure 1D). Nevertheless, we also generated muscle-specific *LAMTOR1* knockout mice (*LAMTOR1*^{MKO}; Figures S1H and S1I) and examined the AMPK p-T172 levels in gastrocnemius muscle from extensively exercised mice. AMPK was also not properly activated in the muscle of *LAMTOR1*^{MKO} mice despite the fact that they displayed similar levels of blood glucose after exercise (Figures 1E and 1F).

We also examined the effect of LAMTOR1 on AMPK activation in cultured cells. Depletion of LAMTOR1 abolished AMPK activation in *LAMTOR1*$^{-/-}$ MEFs or *LAMTOR1*$^{-/-}$ hepatocytes, which were generated by infecting *LAMTOR1*$^{F/F}$ MEF cells or *LAMTOR1*$^{F/F}$ hepatocytes with Cre-expressing adenovirus (Figures 1G and S1K). Reintroduction of LAMTOR1 into *LAMTOR1*$^{-/-}$ MEFs or *LAMTOR1*$^{-/-}$ hepatocytes restored starvation-induced AMPK activation (Figures 1H and S1L). Consistent with a defect in AMPK signaling, *LAMTOR1*^{LKO} mice showed a significant increase in triacylglyeride (TAG) content in the liver upon starvation (Figure S1M) (Assifi et al., 2005), reminiscent of the exacerbated fatty liver in mice infected with si*AXIN*-expressing adenovirus (Zhang et al., 2013). The expression of genes closely related to AMPK activation, *SREBP-1C* (sterol regulatory element-binding protein-1c), *FAS* (fatty acid synthase), and *SCD-1* (stearoyl-CoA desaturase-1) (Li et al., 2011), was deregulated in the *LAMTOR1* knockout liver (Figure S1N). Overall, these results strongly demonstrate that energy stress-induced AMPK signaling is defective in the *LAMTOR1*$^{-/-}$ mouse tissues and cultured cells. The defect in AMPK activation is not a compensatory response to a loss of mTORC1 activity, because the addition of mTORC1 inhibitor rapamycin or Torin1 did not affect the activation of AMPK after glucose starvation (Figures S1O and S1P). In addition to glucose starvation, AMPK can also be stimulated by various other treatments (Gowans et al., 2013; Hawley et al., 2010). The glucose analog 2-DG that elevates the intracellular AMP/ATP ratio (Hawley et al., 2010) activated AMPK in a LAMTOR1-dependent manner (Figures 1I and S1Q), whereas the Ca^{2+} ionophore A23187 used to activate CaMKKβ (Hawley et al., 1995, 2010) did not (Figure 1J), indicating that LAMTOR1 does not exert a role in the CaMKKβ-AMPK pathway. Consistent with a recent report showing that berberine can allosterically activate AMPK (Gowans et al., 2013), we observed increased p-ACC levels in spite of the fact that p-AMPKα levels remained unchanged in *LAMTOR1*$^{-/-}$ MEFs after berberine treatment (Figures S1R and S1S).

It has been well established that LAMTOR1 interacts with LAMTOR2 (P14), LAMTOR3 (MP1), LAMTOR4 (C7ORF59), and

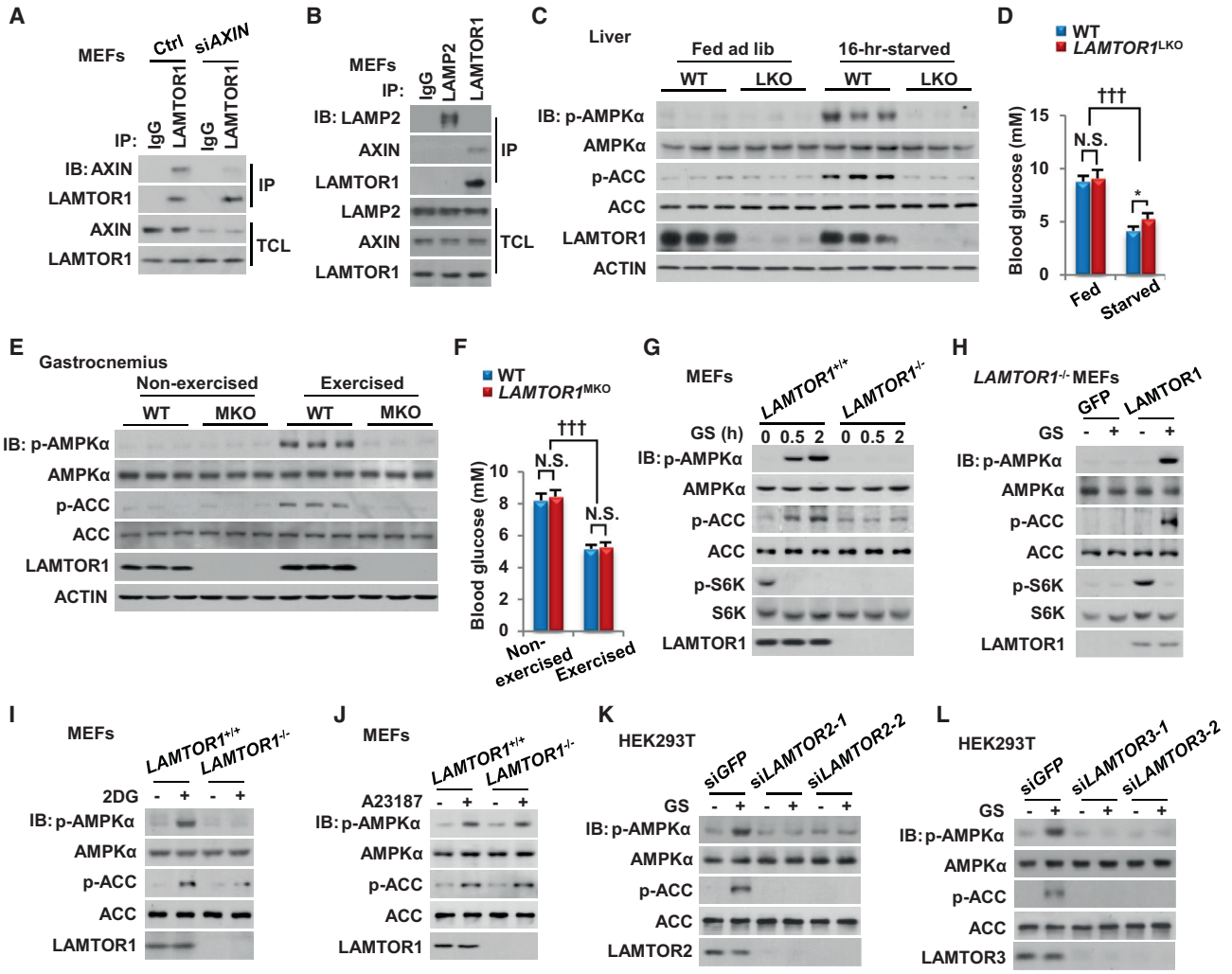

Figure 1. LAMTOR1 Is an AXIN Interactor that Is Required for AMPK Activation upon Energy Stress

(A) Interaction between endogenous AXIN and LAMTOR1. MEFs were infected with Ad-si*AXIN* (si*AXIN*) or Ad-Vector as a control (Ctrl). Immunoprecipitation (IP) was performed and followed by immunoblotting. TCL, total cell lysate.

(B) Interaction between endogenous AXIN, LAMP2, and LAMTOR1.

(C and D) LAMTOR1 deficiency eliminates AMPK activation in mouse liver. Wild-type mice and *LAMTOR1*^{LKO} mice were ad libitum fed or fasted for 16 hr. Liver homogenates were immunoblotted (C) and blood glucose levels were measured (D). Data in (D) are presented as mean ± SEM (n = 8–12 for each condition), *p < 0.05, †††p < 0.001 (ANOVA followed by Tukey). N.S., not significant.

(E and F) LAMTOR1 deficiency eliminates AMPK activation in mouse muscle. Wild-type and *LAMTOR1*^{MKO} mice were at rest or were subjected to maximal exercise. The gastrocnemius muscle homogenates were immunoblotted (E) and blood glucose levels were measured (F). Data in (F) are presented as mean ± SEM (n = 8 for each condition), †††p < 0.001 (ANOVA followed by Tukey). N.S., not significant.

(G) Defective AMPK activation in *LAMTOR1*$^{-/-}$ cells. *LAMTOR1*$^{-/-}$ and *LAMTOR1*$^{+/+}$ MEFs were deprived of glucose for 0.5 or 2 hr. Cells were then lysed and analyzed by immunoblotting. GS, glucose starvation.

(H) Reintroduction of LAMTOR1 into LAMTOR1 null MEFs restores starvation-induced AMPK activation. *LAMTOR1*$^{-/-}$ MEFs stably expressing GFP or ectopic LAMTOR1 were treated and analyzed as described in (G).

(I and J) LAMTOR1 is not involved in the CaMKKβ-AMPK pathway. *LAMTOR1*$^{-/-}$ and *LAMTOR1*$^{+/+}$ MEFs were incubated with 25 mM 2-DG (I), 10 μM A23187 (J), or DMSO for 1 hr. Cells were then lysed and analyzed by immunoblotting.

(K and L) Knockdown of *LAMTOR2* (K) and *LAMTOR3* (L) in HEK293T cells strongly impairs AMPK activation upon energy stress. Cells transfected with siRNA as indicated and glucose starved for 2 hr were lysed and analyzed by immunoblotting.

See also Figure S1.

LAMTOR5 (HBXIP) to form an integral Ragulator complex and that each component is needed for mTORC1 activation (Bar-Peled et al., 2012; Sancak et al., 2010). We thus tested whether the other members in the Ragulator complex also participate in AMPK activation. Indeed, we found that knockdown of *LAMTOR2*, *LAMTOR3*, *LAMTOR4*, or *LAMTOR5* in HEK293T cells all strongly impaired AMPK activation during glucose starvation (Figures 1K, 1L, S1T, and S1U). These results suggest that Ragulator functions as a whole entity in AMPK activation.

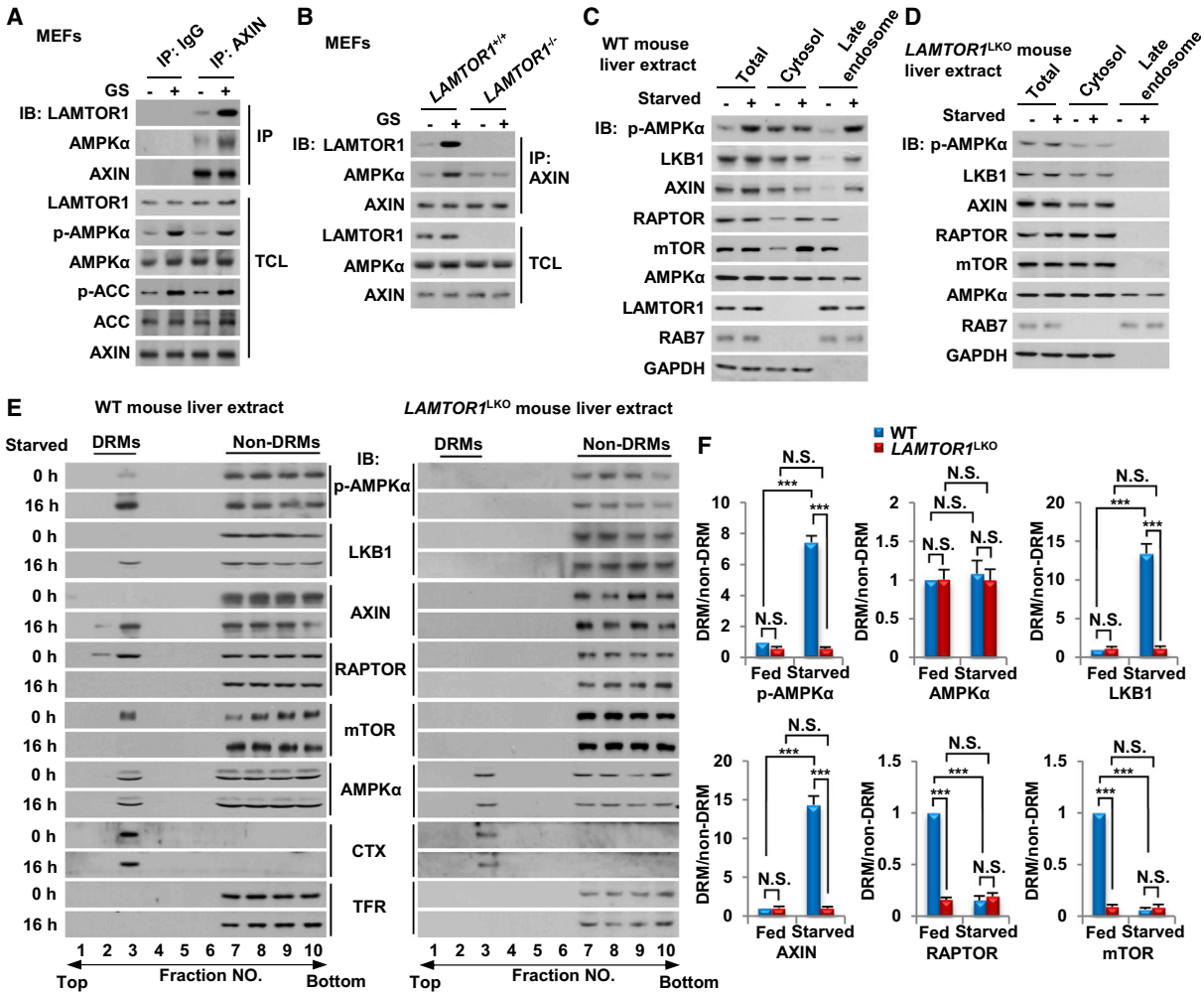

(legend on next page)

Glucose Starvation Induces Ragulator-AXIN/LKB1-AMPK Complex Formation on the Late Endosome

We next investigated the mechanism by which Ragulator controls AMPK activation by analyzing physical interactions between LAMTOR1 and the AXIN/LKB1-AMPK complex. We performed co-IP assays using *LAMTOR1*$^{-/-}$ and *LAMTOR1*$^{+/+}$ MEFs. Endogenous LAMTOR1 and all the other members of Ragulator, along with AMPK, were coprecipitated with AXIN, and the co-IP was increased in glucose-starved (GS) cells (Figures 2A and S2A). A reciprocal IP, by using antibody against LAMTOR1, also revealed an increase in the complex formation of LAMTOR1-AXIN/LKB1-AMPK under starvation (Figure S2B). Knockout of *LAMTOR1* abolished the starvation-enhanced interaction between AMPK and AXIN (Figure 2B). It must be noted here that although we detected AXIN-AMPK interaction after reconstitution of purified AXIN and AMPK before the advent of LAMTOR1, the interaction occurred only after addition of excessively high concentrations of AMP (Zhang et al., 2013). Immunofluorescence staining confirmed that AXIN is colocalized with LAMTOR1 in MEF cells grown in glucose-free medium (Figure S2E); the validation for the antibodies used in immunofluorescent staining are shown in Figure S2C (for AXIN) and Figure S2D (for LAMTOR1).

Since LAMTOR1 is located on the DRM (detergent-resistant membrane, or lipid raft) region of late endosomes/lysosomes (Nada et al., 2009), we next determined whether the complex formation between LAMTOR1 and AXIN/LKB1-AMPK occurs on the late endosomal/DRM surface. We performed subcellular fractionation using mouse liver homogenates by sucrose gradient ultracentrifugation (Gorvel et al., 1991). We also subjected detergent-treated liver or MEF homogenates to sucrose gradient ultracentrifugation and yield DRM and non-DRM fractions (Nada et al., 2009). Dynamic association of the various components with the endosome/DRM before and after starvation were then determined. As expected, LAMTOR1 was detected in the endosome/DRM fraction (Figures 2C, 2E, and S2F). Surprisingly, a significant portion of AMPK was found to be constitutively localized on the late endosome/DRM, as is LAMTOR1 (Figures 2C, 2E, and S2F). However, increased levels of p-AMPK signal induced by starvation were detected only in the late endosome/DRM fractions, in a LAMTOR1-dependent manner (Figures 2C–2E and S2F). AXIN and LKB1 were also detected on LAMTOR1-positive endosomes/DRM, but only after starvation (Figures 2C–2E and S2F). In addition, we found that AXIN (Figure 2G) and LKB1 (Figure S2I; antibody against LKB1 was validated in Figures S2G and S2H) overlapped with the lysosomal marker LAMP2 upon glucose starvation in a LAMTOR1-dependent manner. These results indicate that LAMTOR1 plays an essential role in endosomal localization of AXIN/LKB1 and activation of AMPK upon starvation. Concurrent to AXIN/LKB1 association with the late endosome/DRM during starvation, mTOR and RAPTOR dissociated thereof (Figures 2C, 2E, and S2F). To ascertain the importance of endosomal localization of LAMTOR1 itself for AMPK activation, we reintroduced wild-type LAMTOR1 and endosomal targeting-defective LAMTOR1-3A (Nada et al., 2009) separately into *LAMTOR1*$^{-/-}$ MEFs (Figures S3A and S3B). Unlike wild-type LAMTOR1, LAMTOR1-3A failed to restore AMPK activation or endosomal targeting of AXIN/LKB1 under starvation (Figures 2H, 2I, and S3C–S3E).

The importance of late endosome for AMPK phosphorylation was further underscored by the observation that ectopic expression of RAB5CA (constitutively active form of RAB5) or knockdown of *VPS39* (vacuolar protein sorting 39 homolog), each impeding the maturation of late endosome (Murray et al., 2002; Rink et al., 2005; Stenmark et al., 1994), strongly impaired starvation-induced AMPK activation (Figures 2J and 2K). We then performed in vitro kinase assays to test whether AMPK on the late endosome is functional by mixing endosomes purified as light organelle fractions (Steinberg et al., 2010; Zoncu et al., 2011) as "enzyme" and bacterially expressed GST-ACC1 (aa 34–100) as its substrate (Gowans et al., 2013). The result showed that higher levels of p-AMPK and its kinase activity for ACC were detected on the endosomes from starved cells compared to the

Figure 2. Glucose Starvation Induces Ragulator-AXIN/LKB1-AMPK Complex Formation on the Late Endosome

(A) Glucose deprivation increases the interaction between AXIN, LAMTOR1, and AMPK. Endogenous AXIN in regularly cultured or 2 hr glucose-starved MEFs was immunoprecipitated, followed by immunoblotting.

(B) AXIN interacts with LAMTOR1, and glucose starvation-induced AXIN-AMPK interaction depends on LAMTOR1. Endogenous AXIN in *LAMTOR1*$^{-/-}$ and *LAMTOR1*$^{+/+}$ MEFs was immunoprecipitated and analyzed as described in (A).

(C and D) Starvation-induced increase of p-AMPK and enrichment of AXIN/LKB1 in the late endosome fractions were dependent on LAMTOR1. Liver homogenates from ad libitum fed or 16 hr fasted WT (C) and *LAMTOR1*^{LKO} (D) mice were subjected to sucrose gradient centrifugation. The cytosol and late endosome fractions were collected and analyzed by immunoblotting with antibodies as indicated.

(E) Glucose starvation induces AXIN-LKB1 translocation to detergent-resistant membrane (DRM), with which AMPK and LAMTOR1 are constitutively associated. This effect was abolished in the absence of LAMTOR1. Liver homogenates were treated with Triton X-100 and separated into DRM and non-DRM fractions. Each fraction was analyzed by immunoblotting with antibodies as indicated.

(F) Statistical analysis of (E). Values are presented as mean ± SEM, n = 4, ***$p < 0.001$ (ANOVA followed by Tukey). N.S., not significant.

(G) Glucose deprivation-induced endosomal localization of AXIN depends on LAMTOR1. Goat anti-AXIN antibody and rat anti-LAMP2 antibody were used. Mander's overlap coefficients (MOC) were graphed as mean ± SEM, n = 50–51 for each group, *$p < 1 \times 10^{-12}$ (ANOVA followed by Tukey). N.S., not significant.

(H) The 3A mutation of LAMTOR1 abolishes activation of AMPK or mTORC1. *LAMTOR1*$^{-/-}$ MEFs stably expressing LAMTOR1 or LAMTOR1-3A were deprived of glucose for 2 hr, followed by immunoblotting.

(I) Impaired LAMTOR1-AXIN/LKB1-AMPK complex formation upon starvation in LAMTOR1-3A-expressing MEFs. MEFs were treated as described in (H). Endogenous LAMTOR1 were immunoprecipitated, followed by immunoblotting.

(J) Overexpression of RAB5-CA impairs AMPK activation. HEK293T cells were transfected with plasmids as indicated. Cells were regularly cultured or glucose starved for 2 hr. The immunoprecipitated AMPK were immunoblotted as indicated.

(K) Knockdown of *VPS39* attenuates AMPK activation. HEK293T cells were infected by lentivirus carrying si*GFP* or *VPS39* siRNA. Cells were then glucose starved for 2 hr and lysed. Immunoblotting was then performed.

(L) In vitro phosphorylation of ACC1 by AMPK in the light organelles fraction. Bacterially expressed GST-ACC1 (aa 34–100) was incubated with light organelles purified from regularly cultured or 2 hr glucose-starved *AMPK*$\alpha^{+/+}$ MEFs with 200 μM ATP with or without AMP as indicated, then subjected to immunoblotting. See also Figure S2 and Figure S3.

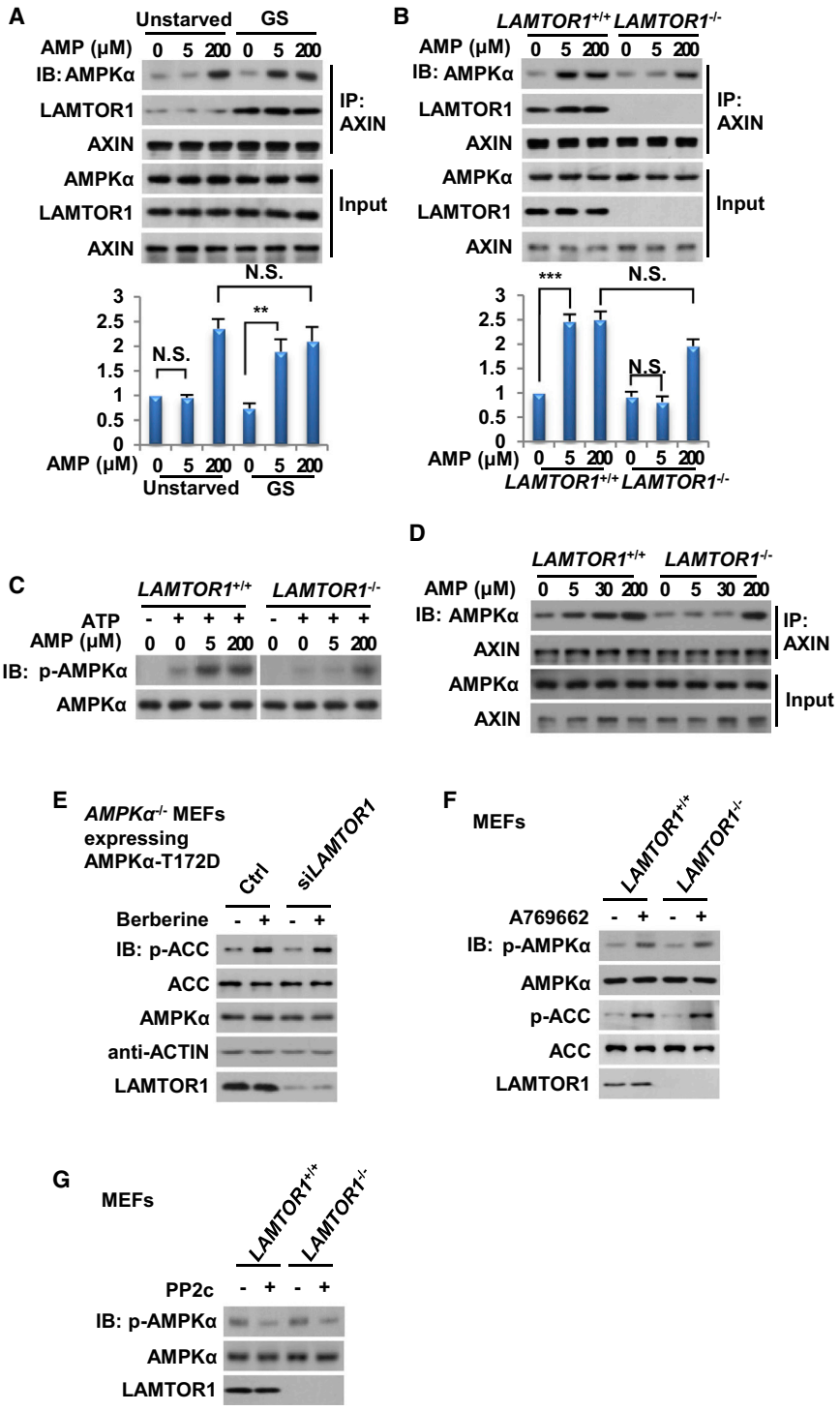

Figure 3. LAMTOR1 Lowers AMP Threshold Concentrations for Stimulation of T172 Phosphorylation of Endosomal AMPK

(A) AMP increases the interaction between AMPK and AXIN on endosome. Crude endosomes purified as light organelles from regularly cultured (unstarved) or 2 hr glucose-starved (GS) MEFs were treated with ODG buffer containing AMP at 0, 5, and 200 μM. The mixtures were immunoprecipitated with antibody against AXIN. The relative amounts of immunoprecipitated AMPKα were calculated from densitometry performed on developed films and normalized to total AMPKα. Data are presented as mean ± SEM, n = 4 for each group, $^{**}p < 0.01$ (ANOVA followed by Tukey). N.S., not significant.

(B) LAMTOR1 lowers the concentration of AMP to induce AXIN-AMPK interaction. Endosome fractions from starved *LAMTOR1*$^{-/-}$ or *LAMTOR1*$^{+/+}$ MEFs were treated and analyzed as described in (A). n = 4 for each group, $^{***}p < 0.001$ (ANOVA followed by Tukey). N.S., not significant.

(C) LAMTOR1 is required for lower concentrations of AMP to induce phosphorylation of AMPKα T172. Crude endosomes were prepared as described in (A). The endosomes were pretreated with PP2C, then terminated by addition of 10 ng/ml okadaic acid, followed by addition with or without 200 μM ATP and AMP as indicated.

(D) LAMTOR1 lowers the concentration of AMP required for inducing AXIN-AMPK interaction in the presence of physiological concentrations of ATP. Endosome fractions were treated and analyzed. The incubation buffer contained 5 mM ATP, with or without AMP as indicated.

(E) Knockdown of *LAMTOR1* does not affect the berberine-induced ACC phosphorylation in *AMPKα*$^{-/-}$ MEFs expressing AMPKα1 T172D mutant. MEFs were infected with adenovirus expressing *GFP* or *LAMTOR1* siRNA and were regularly cultured or glucose-starved for 2 hr, followed by analysis of p-ACC levels.

(F) A769662 activates AMPK in a LAMTOR1-independent manner. MEFs were treated with 100 μM A769662 for 1 hr; cells were then lysed and analyzed by immunoblotting.

(G) Knockout of *LAMTOR1* does not affect the dephosphorylation of AMPK by PP2C. Light organelles were first treated with CaMKKβ for 3 hr and then centrifuged and incubated with PP2C for 1 hr in the presence of 5 μM AMP.

unstarved endosomes, although they both contained similar levels of the AMPK protein (Figures 2L and S3F).

LAMTOR1 Lowers AMP Threshold Concentrations for Stimulation of T172 Phosphorylation of Endosomal AMPK

Before the advent of LAMTOR1, high concentrations of AMP (>150 μM) were needed to promote AMPK interaction with AXIN/LKB1 (Zhang et al., 2013). We wondered whether, in the presence of LAMTOR1, much lower levels of AMP could allow reconstitution of AMPK activation on purified endosomes. We found that as little as 5 μM AMP caused a significant increase in the interaction between AXIN and AMPK as well as T172 phosphorylation using endosomes purified as light organelles from starved wild-type MEFs, but not from starved *LAMTOR1*$^{-/-}$ MEFs (Figures 3A and 3B). In contrast, much higher concentrations (about 200 μM) were required for AMP to promote AXIN-AMPK interaction or T172 phosphorylation on endosomes purified from

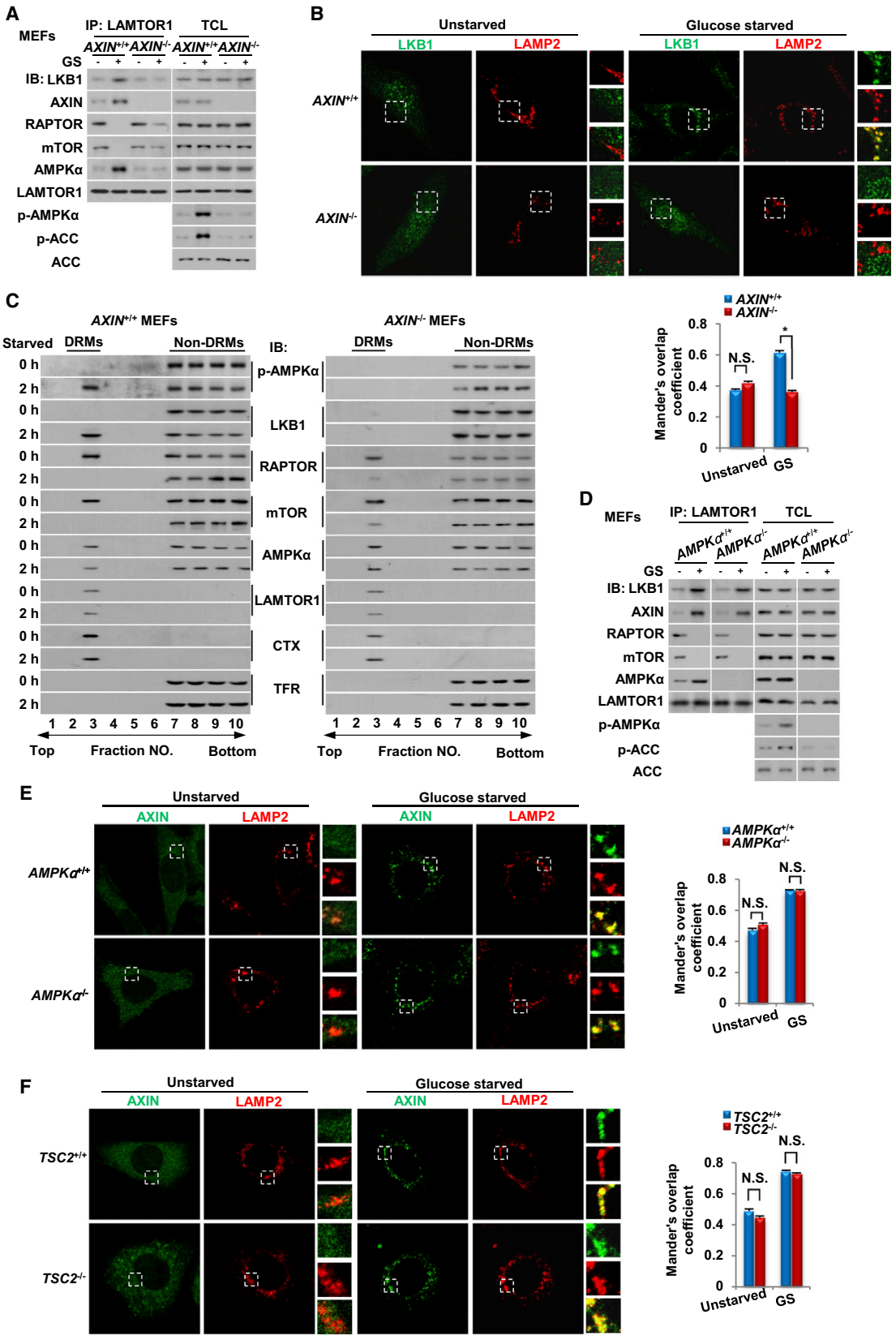

(legend on next page)

starved *LAMTOR1*$^{-/-}$ MEFs or from unstarved wild-type MEFs (Figures 3A–3C). It has been reported that ATP of physiological concentrations (about 5 mM) can strongly influence the AMP sensing of AMPK (Gowans et al., 2013). We hence performed similar assays on AMP dependency of the interaction of AMPK with AXIN by including 5 mM ATP in the reaction. In this case, higher concentrations of AMP (30 μM) were needed for the AXIN-AMPK complex formation on endosomes purified from starved wild-type MEFs, and 200 μM AMP was needed on endosomes purified from starved *LAMTOR1*$^{-/-}$ MEFs (Figure 3D).

Because AMPK can also be activated by AMP through allosteric activation and inhibition of p-T172 dephosphorylation (Carling et al., 1989; Davies et al., 1995), we asked whether LAMTOR1 would participate in these two aspects of AMPK activation. Consistent with previous findings (Gowans et al., 2013), p-ACC levels in *AMPKα*$^{-/-}$ (lacking both AMPKα1 and AMPKα2) MEFs that were reintroduced with an unphosphorylatable AMPK-T172D mutant were dramatically increased after treatment of berberine, indicating that AMPK-T172D can be readily activated, likely due to allosteric changes. However, depletion of LAMTOR1 did not affect the p-ACC level upon treatment of berberine (Figure 3E) or after treatment by A769662, another AMPK allosteric activator (Figure 3F) that acts independently of AMP levels (Hawley et al., 2010). Moreover, we carried out experiments to address whether LAMTOR1 affects dephosphorylation of AMPK by incubating endosomes purified from starved wild-type or *LAMTOR1*$^{-/-}$ MEFs with CaMKKβ to yield fully T172 phosphorylated AMPK, followed by centrifugation to remove CaMKKβ. The endosomes were then treated with PP2C, followed by monitoring p-T172 levels. The results show that loss of LAMTOR1 does not affect p-T172 dephosphorylation, either (Figure 3G). These results suggest that the newly identified AXIN-Ragulator-AMPK axis operates to induce LKB1-mediated AMPK activation, but is not involved in direct allosteric activation, inhibition of dephosphorylation, reconciling well with the current models of AMPK activation that can be achieved through three different ways (Gowans et al., 2013).

V-ATPase and Ragulator Together Act as a Primary Sensor to Facilitate the Endososomal Translocation of AXIN/LKB1

We next directly addressed the tethering role of AXIN in LKB1 translocation by using *AXIN* knockout cells. We generated *AXIN*-floxed mice and *AXIN*$^{F/F}$ MEFs (Figures S4A–S4C). When assessed by co-IP assay using the lysates from *AXIN*$^{-/-}$ MEFs (by infecting *AXIN*$^{F/F}$ MEFs with Ad-Cre adenovirus), starvation-induced increase in the complex formation of LKB1, AMPK, and LAMTOR1 or in the phosphorylation of AMPKα was attenuated (Figures 4A–4C), indicating that AXIN indeed plays a scaffolding role in starvation-triggered translocation of LKB1 to endosome.

We then set out to determine the initiating step that enables the endosomal translocation of AXIN/LKB1 during starvation. It was found that AXIN/LKB1 was properly translocated to the endosome in *AMPKα*$^{-/-}$ MEFs (Figures 4D, 4E, S4D, and S4E), ruling out the possibility that AMPK facilitates this process. We also tested whether TSC2 has a role in AXIN/LKB1 endosomal translocation using *TSC2*$^{-/-}$ MEFs, showing again that TSC2 does not change the efficiency of AXIN/LKB1 translocation in response to starvation (Figures 4F and S4F–S4H). However, this raised the issue of which molecule is responsible for sensing energy stress to trigger assembly of the AMPK-activating complex on the endosome. It was previously shown that Ragulator is regulated by the energy sensor v-ATPase in response to glucose starvation (Efeyan et al., 2013). We thus tested the possibility that v-ATPase may also be a triggering sensor for AMPK activation. We found that the increased interaction between AXIN/LKB1 and LAMTOR1 or the enrichment of AXIN/LKB1 on DRM upon glucose deprivation was strongly impaired in the absence of functional v-ATPase when its *V0C* subunit (*ATP6V0C*) was knocked down (Figures 5A and 5B). Levels of p-T172 were not increased after glucose starvation in *ATP6V0C* knockdown cells (Figure 5A). As expected, mTOR/RAPTOR association with LAMTOR1 or DRM from cells was also diminished in v-ATPase-deficient cells cultured in the normal condition (Figures 5A and 5B), indicating that v-ATPase is required for the endosomal translocation of AXIN/LKB1 and AMPK T172 phosphorylation during glucose starvation. Consistently, in cells treated with the v-ATPase inhibitor Concanamycin A (ConA), which mimics starvation-induced inhibition of v-ATPase (Efeyan et al., 2013; Zoncu et al., 2011), more AXIN/LKB1 translocated to the endosome (Figures 5C and S5A) and interacted with LAMTOR1 (Figure S5B). We then reconstituted the endosomal translocation of AXIN/LKB1 by using light organelles isolated from differently treated cells. AXIN, bacterially expressed or from the cytosol of unstarved cells, showed a stronger interaction with LAMTOR1 when mixed with light organelles isolated from ConA-treated or glucose-starved cells (Figures 5D and 5E). These results indicate that inhibition of v-ATPase during glucose starvation is able to induce, and is necessary for, the endosomal translocation of AXIN/LKB1. Interestingly, we found that AXIN interacted with v-ATPase, and importantly, this interaction was increased upon glucose starvation (Figure 5F). Moreover, glucose starvation and ConA treatment also induced the

Figure 4. AXIN Plays a Scaffolding Role in Starvation-Triggered Translocation of LKB1 to Endosome

(A) AXIN is required for LAMTOR1 to form a complex with AMPK and LKB1. Endogenous LAMTOR1 in regularly cultured or 2 hr glucose-starved *AXIN*$^{-/-}$ and *AXIN*$^{+/+}$ MEFs was immunoprecipitated, followed by immunoblotting.

(B) AXIN is required for glucose deprivation-induced endosomal localization of LKB1. Cells were incubated with culture medium deprived of glucose for 3 hr. Rabbit anti-LKB1 antibody and rat anti-LAMP2 antibody were used. MOC was graphed as mean ± SEM, n = 49–51 for each group, *$p < 1 \times 10^{-12}$ (ANOVA followed by Tukey). N.S., not significant.

(C) AXIN is required for the increase of p-AMPK levels and enrichment of LKB1 on the DRM fractions. Cells were cultured in glucose-free medium for 2 hr, followed by sucrose gradient centrifugation as described in Figure 2E.

(D) Intact AMPK-AXIN/LKB1-LAMTOR1 complex formation upon starvation in *AMPKα*$^{-/-}$ MEFs. Cells were treated and analyzed as described in (A).

(E and F) Glucose deprivation-induced endosomal localization of AXIN was intact in *AMPKα*$^{-/-}$ (E) or *TSC2*$^{-/-}$ (F) MEFs. Cells were treated and analyzed as described in Figure 2G. The values of MOC were graphed as mean ± SEM, n = 47–52 (E) and n = 46–51 (F) for each group. N.S., not significant.

See also Figure S4.

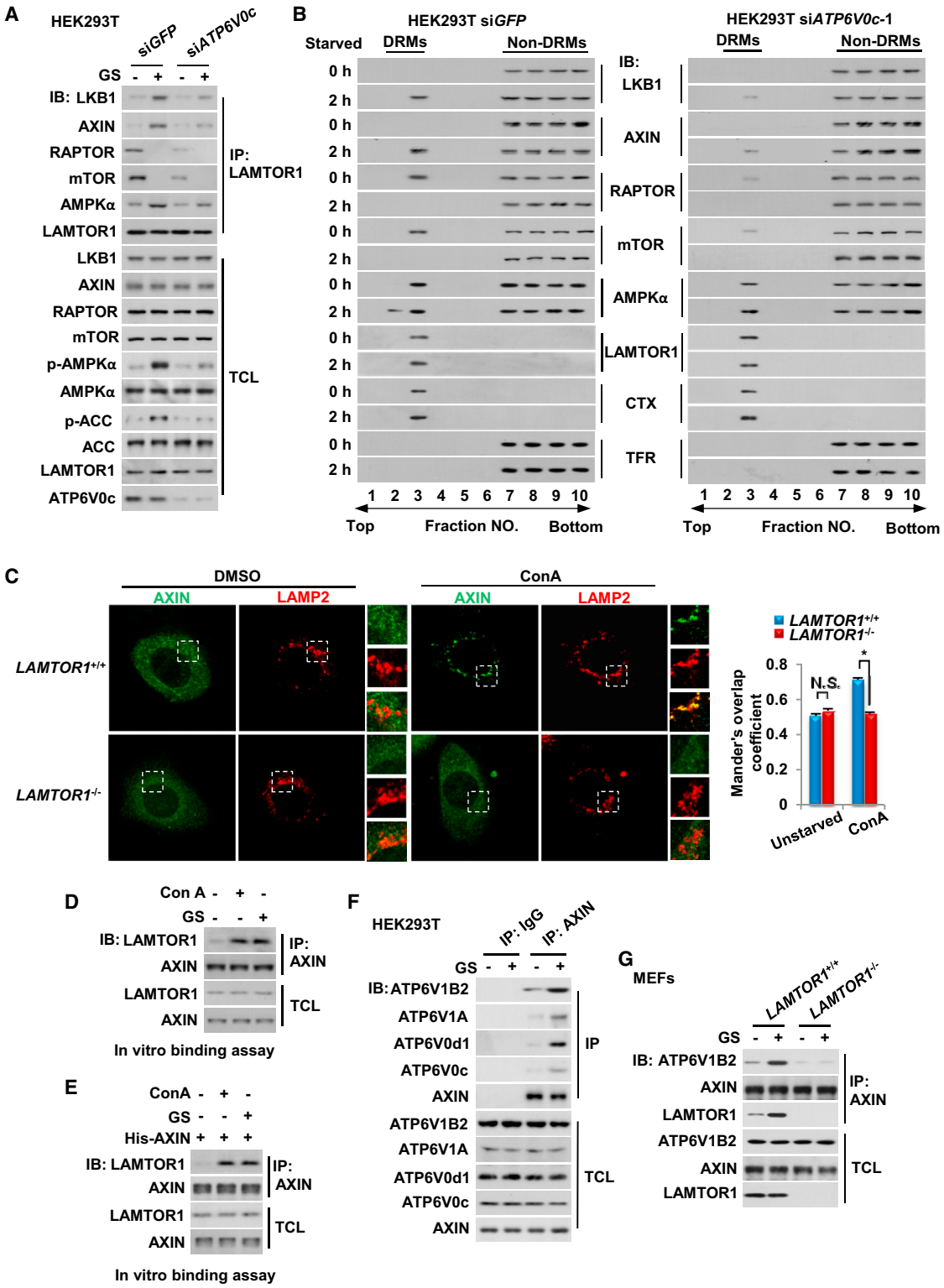

Figure 5. V-ATPase and Ragulator Together Act as Primary Sensors to Facilitate Endososomal Translocation of AXIN/LKB1

(A) Knockdown of *ATP6V0C* attenuated glucose starvation-induced interaction between AXIN/LKB1 and LAMTOR1. HEK293T cells transfected with siRNA targeting *ATP6V0C*, or *GFP* as a control, were deprived of glucose for 2 hr. Endogenous LAMTOR1 was immunoprecipitated, followed by immunoblotting.

(B) Knockdown of *ATP6V0C* dampened the DRM localization of AXIN and LKB1 upon glucose starvation. HEK293T cells were treated as described in (A), then subjected to subcellular fractionation to yield DRM and non-DRM fractions.

(legend continued on next page)

AXIN-v-ATPase interaction and endosomal translocation of AXIN/LKB1, which was abrogated in cells lacking the LAMTOR1 subunit of Ragulator (Figures 5C and 5G; Figure S5A). We also examined the other four subunits of Ragulator and found that knockdown of them diminished the interaction between AXIN and v-ATPase (Figures S5C–S5F), pointing to a requirement of an intact Ragulator complex for endosomal translocation of AXIN and AMPK activation (Figures 1K and 1L; Figures S1O and S1P). These results indicate that v-ATPase and Ragulator together act as primary sensors and provide docking sites for AXIN/LKB1.

By contrast, although RAGs can interact with Ragulator, they are not involved in endosomal translocation of AXIN, as knockdown of *RAG*s affected neither AMPK activation nor the interaction between LAMTOR1 and AXIN (Figure S5G). Similarly, $RAGB^{GTP}$, a constitutively GTP-bound form of RAGB (Sancak et al., 2008), did not affect LAMTOR1-AXIN interaction (Figure S5H), consistent with an earlier report that $RAGB^{GTP}$ has no impact on AMPK activation (Efeyan et al., 2013).

AXIN Facilitates v-ATPase Inhibition-Triggered Dissociation of mTOR from Endosome

It is highly intriguing that the physiologically antagonistic AMPK and mTOR share the same activating factors, v-ATPase and Ragulator. It stands to reason that there exists a fine mechanism centered on v-ATPase-Ragulator that governs translocation of AXIN/LKB1 or the mTORC1 complex onto the endosomal surface. We thus examined whether and how AXIN may facilitate mTORC1 dissociation from endosome upon glucose starvation. Indeed, depletion of AXIN strongly slowed down the dissociation of mTOR from endosome/DRM (Figures 6A and 4C; antibody against mTOR validated in Figures S6A and S6B) and the decrease of mTORC1 activity (by assessing p-S6K levels) upon glucose deprivation (Figure S6C). Similarly, ConA-induced endosomal dissociation of mTORC1 was also strongly attenuated in $AXIN^{-/-}$ MEFs (Figure 6B). We also evaluated whether TSC2 and AMPK participate in the AXIN-mediated mTORC1 suppression. In $TSC2^{-/-}$ MEFs and $AMPK\alpha^{-/-}$ MEFs, the dissociation of mTOR from the endosome (Figures S6D and S6E) and decreasing of p-S6K levels (Figures 6C and 6D) were still observed upon glucose starvation. When *AXIN* was knocked down in these cells, dissociation of mTOR from the endosome (Figures S6D and S6E) or decrease of p-S6K levels (Figures 6C and 6D) was attenuated. As one previous study implicated GSK3 in the suppression of mTORC1 (Inoki et al., 2006), we also treated $AXIN^{-/-}$ and $AXIN^{+/+}$ MEFs with the GSK3 inhibitor SB216763 and found that GSK3 inhibition did not affect mTORC1 endosomal dissociation or p-S6K levels (Figure S6F). Overall, these results suggest that it is AXIN that plays an essential role in mediating starvation-triggered endosomal dissociation and inhibition of mTORC1.

We then mapped the region of AXIN responsible for interacting with LAMTOR1, revealing that its N-terminal region (aa 1–400; AXIN-NT) encompasses the interaction interface for LAMTOR1 (Figures S6G and S6H). AXIN-NT acted as a dominant-negative form for AMPK activation due to its lacking the C-terminal LKB1 binding domain (Figure 6E). Intriguingly, AXIN-NT unbiasedly localized to late endosome and interacted with LAMTOR1 as well as v-ATPase on DRM regardless of glucose starvation (Figures 6E, 6F, and S6I). In addition, reintroduction of AXIN-NT into AXIN null MEFs strongly hindered the binding of mTORC1 to DRM and prevented mTORC1 activation (Figures 6E, 6G, and S6J) in regularly cultured cells. This observation indicates that AXIN-NT is constitutively active in binding to Ragulator and is efficient in dissociating mTORC1 from endosome, independently of starvation signal in cells. We then reconstituted this process in vitro. AXIN-NT, but not full-length AXIN from unstarved cells, effectively dissociated mTORC1 from the endosomes purified from unstarved cells (Figure 6H). All these lines of evidence point to a scenario that glucose starvation changes the conformation of v-ATPase-Ragulator complex (Efeyan et al., 2013) that "activates" AXIN to further associate with the v-ATPase-Ragulator complex, which in turn further induces the complex to undergo conformational changes, ultimately leading to mTORC1 dissociation from endosome.

AXIN Binding Inhibits the GEF Activity of Ragulator toward RAGs

Finally, we analyzed the mechanisms by which AXIN facilitates mTOR dissociation from endosome upon starvation. It has been known that endosomal localization of mTOR is directly influenced by the RAGs, in that nutrient starvation converts RAGs to their GDP-bound form that exhibits higher affinity for Ragulator instead of mTORC1 (Bar-Peled et al., 2012; Sancak et al., 2008, 2010; Zoncu et al., 2011). We found that knockout of *AXIN* attenuated the enhancement of Ragulator-RAG interaction induced by glucose starvation (Figure 7A), and that AXIN-NT sufficiently enhanced the interaction between RAGs and Ragulator in unstarved cells (Figures 7B and S7A), indicating that AXIN binding to Ragulator can increase its affinity for RAGs. However, AXIN did not directly interact with RAGs (Figure 7C). We hence tested whether AXIN affects the nucleotide binding state of RAGs. It was found that even AXIN-NT could not facilitate dissociation of mTORC1 in 293T cells expressing $RAGB^{GTP}$ that constitutively binds GTP (Figure 7D). To test for a possible effect of AXIN on the GEF activity of Ragulator, we carried out in vitro reconstitution and showed that AXIN-NT indeed strongly dampened the GEF activity of Ragulator toward RAGB (Figures 7E and

(C) ConA induces endosomal translocation of AXIN in a LAMTOR1-dependent manner. MEFs were treated with 5 μM ConA or DMSO as a control for 2 hr and then analyzed as described in Figure 2G. MOC of was graphed as mean ± SEM, n = 49–53 for each group, *$p < 1 \times 10^{-12}$ (ANOVA followed by Tukey). N.S., not significant.

(D and E) Reconstitution of the endosomal translocation process. Unstarved AXIN-containing cytosol (D) or bacterially expressed His-AXIN (E) was mixed with light organelles purified from unstarved, 2 hr glucose-starved or 5 μM ConA-treated cells. The mixtures were then lysed and endogenous LAMTOR1 was immunoprecipitated.

(F) Glucose deprivation increases the interaction between AXIN and v-ATPase. Endogenous AXIN in regularly cultured or 2 hr glucose-starved HEK293T cells was immunoprecipitated. The immunoprecipitates were then subjected to immunoblotting with antibodies as indicated.

(G) Knockout of *LAMTOR1* abolishes the interaction between AXIN and v-ATPase. MEFs were treated and analyzed as described in (F).

See also Figure S5.

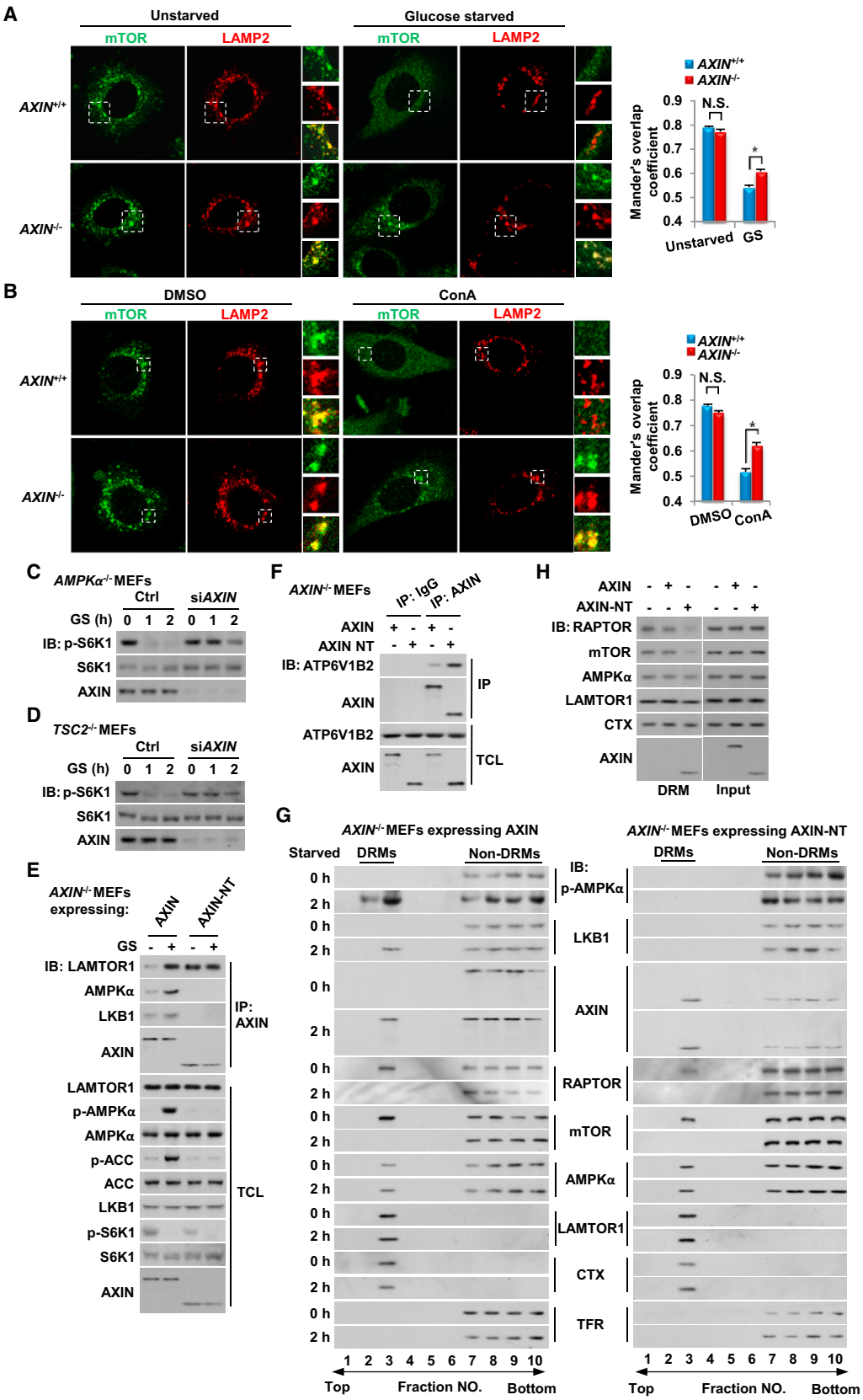

(legend on next page)

S7B), similar to the functional mode for mTORC1 regulation (Efeyan et al., 2013; Menon et al., 2014; Settembre et al., 2013; Zoncu et al., 2011); however, AXIN did not affect the interaction between v-ATPase and Ragulator per se upon glucose starvation (Figure 7A). We also tested for any role of AXIN in the regulation of mTORC1 activity by amino acid signaling and found that AXIN does not take part in this process (Figure S7C), indicating that AXIN specifically regulates the route from energy stress to mTORC1 inhibition.

DISCUSSION

Through targeted gene deletion or knockdown approaches, we have found that the endosomal proteins v-ATPase and Ragulator, known to be required for mTORC1 activation when nutrient supply is abundant, are also essential in LKB1-mediated AMPK activation in response to energy stress. It appears that all the components of Ragulator, LAMTOR1–LAMTOR5, are required for the activation of AMPK. Under energy stress, LKB1-bound AXIN translocates to the endosomal surface and interacts with the v-ATPase-Ragulator complex, in addition to AMP-bound AMPK that is also a residential endosomal protein. It is on the endosomal surface that LKB1 phosphorylates AMPK.

Therefore, the v-ATPase-Ragulator complex serves as a dual sensor for energy/nutrient sufficiency and deficiency, depending on which signal is prevailing. Starvation elicits an initiating signal originated as a result of conformational changes of the sensor complex, which favors docking of AXIN/LKB1 to allow for AMPK activation. Importantly, once AXIN anchors to the docking sites consisting of v-ATPase, Ragulator, and AMP-bound AMPK, it dissociates mTORC1 through inhibiting the GEF activity of the Ragulator complex toward RAGs, thereby forming a pivot for the switch between procatabolic and proanabolic pathways (Figure 7F). Moreover, our findings emphasize a general role of late endosome/lysosome in controlling metabolic programs.

EXPERIMENTAL PROCEDURES

Mouse Exercise Studies, Cell Culture, Transient Transfection, and Lentivirus Infection

Mouse exercise studies were performed as described previously (He et al., 2012). HEK293T and MEFs were maintained in Dulbecco's modified Eagle's medium (DMEM). Polyethylenimine was used to transfect HEK293T cells. Transfected cells were harvested 24 hr after transfection. Lentivirus for infection of the MEFs was packaged in HEK293T cells using Lipofectamine 2000. Cells were trypsinized and replated at 24 hr after virus infection. *LAMTOR1*$^{F/F}$, *AXIN*$^{F/F}$, and *LKB1*$^{F/F}$ MEFs were established by introducing SV40 T antigen into primary cultured embryonic cells from a litter of *LAMTOR1*$^{F/F}$, *AXIN*$^{F/F}$, or *LKB1*$^{F/F}$ mice. *LAMTOR1*$^{-/-}$ and *AXIN*$^{-/-}$ MEFs were generated by infecting *LAMTOR1*$^{F/F}$, *AXIN*$^{F/F}$, and *LKB1*$^{F/F}$ MEFs with Ad-Cre adenoviruses. MEFs stably expressing LAMTOR1, LAMTOR1-3A, AXIN, or AXIN-NT were established by infecting *LAMTOR1*$^{F/F}$ and *AXIN*$^{F/F}$ MEFs with respective lentivirus-based constructs, followed by infection with Ad-Cre to deplete LAMTOR1 or AXIN. All animal experiments were approved by the Institutional Animal Care and Use Committee at Xiamen University.

Immunoprecipitation and Immunoblotting

Cell lysis and IP were carried out as described previously (Rui et al., 2004; Zhang et al., 2013), with some modifications. Dishes of MEFs (10 × 15 cm dishes for immunoprecipitating LAMTOR1 and 4 × 15 cm dishes for immunoprecipitating AXIN in each lane) were collected and lysed with ODG buffer (50 mM Tris-HCl [pH 8.0], 50 mM NaCl, 1 mM EDTA, 1 mM EGTA, 2% ODG, 5 mM β-mercaptoethanol with protease inhibitor cocktail). Cell lysates were incubated with respective antibodies overnight. Levels of total proteins and the levels of phosphorylation of proteins were analyzed on separate gels. The band intensities on developed films were quantified using ImageJ software (NIH).

Immunofluorescence Assays

Cells were cultured on glass coverslips in six-well tissue culture dishes and were fixed with 4% formaldehyde in phosphate-buffered saline (PBS) at room temperature (RT). The slides were rinsed twice with PBS and cells were permeabilized with 0.1% Triton X-100 in PBS (except for staining mTOR with 0.05% Triton X-100) for 5 min at 4°C. After rinsing twice with PBS, the slides were incubated with primary antibody diluted in PBS overnight at 4°C, rinsed four times with PBS, and incubated with secondary antibodies for 7–8 hr at RT in the dark. The slides were washed four times with PBS, then mounted on glass coverslips and imaged on a Zeiss Laser Scanning Microscope (LSM) 780. For quantitative analyses, threshold Pearson's correlation coefficients and colocalization percentages (determined by Mander's overlap coefficient) were calculated by ZEN 2010 software (Zeiss). For each condition, ~50 cells were analyzed.

Subcellular Fractionation and Nucleotide Exchange Assays

Late endosomal fractions were prepared as described (Gorvel et al., 1991). DRM and non-DRM fractions were separated as described previously (Nada et al., 2009). Light organelles were purified as described previously (Steinberg et al., 2010; Zoncu et al., 2011). Nucleotide exchange assays were performed as described previously (Bar-Peled et al., 2012).

Statistical Analyses

ANOVA with Tukey's post test was used to compare values among different experimental groups using the SPSS Statistics 17.0 program. For experiments

Figure 6. AXIN Facilitates v-ATPase Inhibition-Triggered Dissociation of mTOR from Endosome

(A) Immunostaining analysis of AXIN dependency of glucose deprivation-induced dissociation of mTOR from endosome. *AXIN*$^{-/-}$ MEFs and *AXIN*$^{+/+}$ MEFs were cultured in glucose-deprived medium for 2 hr. Rabbit anti-mTOR antibody and rat anti-LAMP2 antibody were used. MOC was graphed as mean ± SEM, n = 50–52 for each group, *$p < 1 \times 10^{-6}$ (ANOVA followed by Tukey). N.S., not significant.

(B) Knockout of AXIN attenuates ConA-driven dissociation of mTOR from endosome. *AXIN*$^{-/-}$ and *AXIN*$^{+/+}$ MEFs were treated with 5 μM ConA or DMSO as a control for 2 hr, then analyzed as described in (A). MOC was graphed as mean ± SEM, n = 51–58 for each group, *$p < 1 \times 10^{-11}$ (ANOVA followed by Tukey). N.S., not significant.

(C and D) Knockdown of *AXIN* slows down the inhibition of mTORC1 activity after glucose starvation in *AMPKα*$^{-/-}$ (C) and *TSC2*$^{-/-}$ (D) MEFs. Cells were infected with Ad-si*AXIN* (si*AXIN*) or Ad-Vector as a control (Ctrl) and were then subjected to glucose starvation for 1 or 2 hr. p-S6K levels were analyzed by immunoblotting.

(E) AXIN-NT (aa 1–400) lacking LKB1 binding domain exerts a dominant-negative effect on AMPK activation and effectively inhibits mTOR activity. *AXIN*$^{-/-}$ MEFs stably expressing AXIN or AXIN-NT were regularly cultured or glucose starved for 2 hr and were subjected to immunoprecipitation with antibody against AXIN.

(F) AXIN-NT constitutively interacts with v-ATPase. Cells were lysed and AXIN was then immunoprecipitated.

(G) AXIN-NT is constitutively detected on DRM. Lysates of starved or unstarved cells were separated into DRM and non-DRM fractions, followed by immunoblotting as indicated.

(H) AXIN-NT (aa 1–400) constitutively dissociates mTORC1 from endosome. Cytosol fractions of indicated unstarved MEFs were prepared and mixed with the endosomes purified from unstarved WT MEFs. The mixtures were then subjected to DRM preparation and analyzed by immunoblotting.

See also Figure S6.

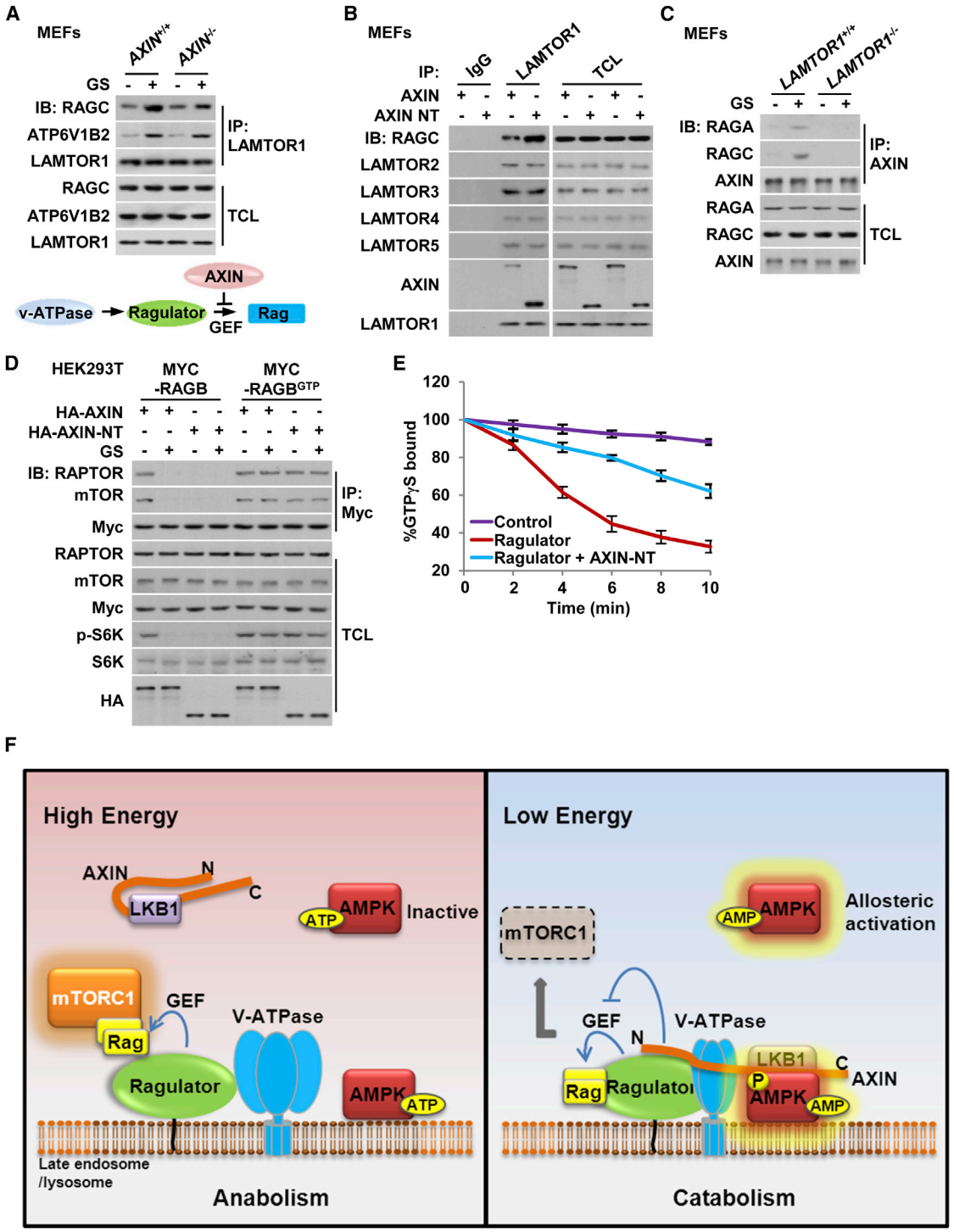

Figure 7. AXIN Binding Inhibited the GEF Activity of Ragulator toward RAGs

(A) Knockout of *AXIN* attenuates starvation-induced interaction between RAG and Ragulator, but not the interaction between v-ATPase and Ragulator. MEFs were cultured in glucose-deprived medium for 2 hr. Endogenous LAMTOR1 was immunoprecipitated. The results are further illustrated in the schematic diagram below.

(B) AXIN-NT enhances the interaction between Ragulator and RAGs. MEFs were lysed and LAMTOR1 was immunoprecipitated.

(C) AXIN interacts with RAG in a LAMTOR1-dependent manner. Endogenous AXIN in regularly cultured or 2 hr glucose-starved *LAMTOR1*$^{-/-}$ and *LAMTOR1*$^{+/+}$ MEFs was immunoprecipitated.

(D) AXIN functions upstream of RAG. HEK293T cells stably expressing Myc-RAGB or Myc-RAGB^{GTP} were transfected with HA-AXIN or HA-AXIN-NT. Cells were regularly cultured or deprived of glucose for 2 hr, then immunoprecipitated with antibody against Myc-tag.

(legend continued on next page)

with only two groups, Student's t test was used as specified in the figure legends.

Additional Experimental Procedures

Additional experimental procedures are provided in the Supplemental Information.

SUPPLEMENTAL INFORMATION

Supplemental Information includes Supplemental Experimental Procedures and seven figures and can be found with this article online at http://dx.doi.org/10.1016/j.cmet.2014.06.014.

AUTHOR CONTRIBUTIONS

C.-S.Z., B.J., M.L. and S.-C.L. conceived the project. C.-S.Z. performed most cellular experiments with assistance from M.L., and B.J. performed most animal experiments. S.-Y.L., Y.P., Y.-L.Z., M.Z., Y.-Q.W., T.Y.L., Y.L., Z.L., G.L., Q.L., H.Y., and H.G. performed experiments and participated in discussion of the results. Z. Yin, Z. Ye, J.H., J.-W.W., T.Y.L., and S.-Y.L. helped with discussion and interpretation of results. S.-C.L. and S.-Y.L. wrote the manuscript. S.-C.L., J.-W.W., and J.H. edited the manuscript.

ACKNOWLEDGMENTS

We thank Drs. B. Viollet and K.R. Laderoute for providing *AMPK*$\alpha^{-/-}$ MEFs and Dr. Hongbing Zhang for providing *TSC2*$^{-/-}$ MEFs. This work was supported by grants from National Natural Science Foundation of China (#31130016), the 973 Program (#2011CB910800, #2013CB530600, and #2014CB910602), and additional grants from National Natural Science Foundation of China (#31221065 and #31300626).

Received: April 23, 2014
Revised: May 19, 2014
Accepted: June 23, 2014
Published: July 3, 2014

REFERENCES

Assifi, M.M., Suchankova, G., Constant, S., Prentki, M., Saha, A.K., and Ruderman, N.B. (2005). AMP-activated protein kinase and coordination of hepatic fatty acid metabolism of starved/carbohydrate-refed rats. Am. J. Physiol. Endocrinol. Metab. *289*, E794–E800.

Bai, X.C., Ma, D.Z., Liu, A.L., Shen, X.Y., Wang, Q.J.M., Liu, Y.J., and Jiang, Y. (2007). Rheb activates mTOR by antagonizing its endogenous inhibitor, FKBP38. Science *318*, 977–980.

Bar-Peled, L., Schweitzer, L.D., Zoncu, R., and Sabatini, D.M. (2012). Ragulator is a GEF for the rag GTPases that signal amino acid levels to mTORC1. Cell *150*, 1196–1208.

Bar-Peled, L., Chantranupong, L., Cherniack, A.D., Chen, W.W., Ottina, K.A., Grabiner, B.C., Spear, E.D., Carter, S.L., Meyerson, M., and Sabatini, D.M. (2013). A Tumor suppressor complex with GAP activity for the Rag GTPases that signal amino acid sufficiency to mTORC1. Science *340*, 1100–1106.

Carling, D., Clarke, P.R., Zammit, V.A., and Hardie, D.G. (1989). Purification and characterization of the AMP-activated protein kinase. Copurification of acetyl-CoA carboxylase kinase and 3-hydroxy-3-methylglutaryl-CoA reductase kinase activities. Eur. J. Biochem. *186*, 129–136.

Carling, D., Thornton, C., Woods, A., and Sanders, M.J. (2012). AMP-activated protein kinase: new regulation, new roles? Biochem. J. *445*, 11–27.

Chen, L., Jiao, Z.H., Zheng, L.S., Zhang, Y.Y., Xie, S.T., Wang, Z.X., and Wu, J.W. (2009). Structural insight into the autoinhibition mechanism of AMP-activated protein kinase. Nature *459*, 1146–1149.

Davies, S.P., Helps, N.R., Cohen, P.T.W., and Hardie, D.G. (1995). 5′-AMP inhibits dephosphorylation, as well as promoting phosphorylation, of the AMP-activated protein kinase. Studies using bacterially expressed human protein phosphatase-2C alpha and native bovine protein phosphatase-2AC. FEBS Lett. *377*, 421–425.

Dibble, C.C., and Manning, B.D. (2013). Signal integration by mTORC1 coordinates nutrient input with biosynthetic output. Nat. Cell Biol. *15*, 555–564.

Efeyan, A., Zoncu, R., Chang, S., Gumper, I., Snitkin, H., Wolfson, R.L., Kirak, O., Sabatini, D.D., and Sabatini, D.M. (2013). Regulation of mTORC1 by the Rag GTPases is necessary for neonatal autophagy and survival. Nature *493*, 679–683.

Gorvel, J.P., Chavrier, P., Zerial, M., and Gruenberg, J. (1991). rab5 controls early endosome fusion in vitro. Cell *64*, 915–925.

Gowans, G.J., Hawley, S.A., Ross, F.A., and Hardie, D.G. (2013). AMP is a true physiological regulator of AMP-activated protein kinase by both allosteric activation and enhancing net phosphorylation. Cell Metab. *18*, 556–566.

Gwinn, D.M., Shackelford, D.B., Egan, D.F., Mihaylova, M.M., Mery, A., Vasquez, D.S., Turk, B.E., and Shaw, R.J. (2008). AMPK phosphorylation of raptor mediates a metabolic checkpoint. Mol. Cell *30*, 214–226.

Hardie, D.G., Ross, F.A., and Hawley, S.A. (2012). AMPK: a nutrient and energy sensor that maintains energy homeostasis. Nat. Rev. Mol. Cell Biol. *13*, 251–262.

Hawley, S.A., Selbert, M.A., Goldstein, E.G., Edelman, A.M., Carling, D., and Hardie, D.G. (1995). 5′-AMP activates the AMP-activated protein kinase cascade, and Ca2+/calmodulin activates the calmodulin-dependent protein kinase I cascade, via three independent mechanisms. J. Biol. Chem. *270*, 27186–27191.

Hawley, S.A., Boudeau, J., Reid, J.L., Mustard, K.J., Udd, L., Mäkelä, T.P., Alessi, D.R., and Hardie, D.G. (2003). Complexes between the LKB1 tumor suppressor, STRAD alpha/beta and MO25 alpha/beta are upstream kinases in the AMP-activated protein kinase cascade. J. Biol. *2*, 28.

Hawley, S.A., Ross, F.A., Chevtzoff, C., Green, K.A., Evans, A., Fogarty, S., Towler, M.C., Brown, L.J., Ogunbayo, O.A., Evans, A.M., and Hardie, D.G. (2010). Use of cells expressing gamma subunit variants to identify diverse mechanisms of AMPK activation. Cell Metab. *11*, 554–565.

He, C.C., Bassik, M.C., Moresi, V., Sun, K., Wei, Y., Zou, Z., An, Z., Loh, J., Fisher, J., Sun, Q., et al. (2012). Exercise-induced BCL2-regulated autophagy is required for muscle glucose homeostasis. Nature *481*, 511–515.

Inoki, K., Li, Y., Zhu, T.Q., Wu, J., and Guan, K.L. (2002). TSC2 is phosphorylated and inhibited by Akt and suppresses mTOR signalling. Nat. Cell Biol. *4*, 648–657.

Inoki, K., Ouyang, H., Zhu, T., Lindvall, C., Wang, Y., Zhang, X., Yang, Q., Bennett, C., Harada, Y., Stankunas, K., et al. (2006). TSC2 integrates Wnt

(E) AXIN-NT inhibits the GEF activity of Ragulator toward RAGB. RagB-RagC^{D181N}, which is used to analyze the nucleotide binding and exchanging of RAGB (Bar-Peled et al., 2012), was loaded with [^{35}S]GTPγS and incubated with Ragulator or AXIN-NT as indicated. Dissociation was monitored by a filter-binding assay. Each value represents the normalized mean ± SD, n = 5.
(F) A simplified model depicting that v-ATPase-Ragulator is an initiating sensor complex for switch between AMPK and mTOR activation. When nutrients are abundant, the "active" v-ATPase stimulates the GEF activity of Ragulator toward Rags and activates mTORC1. Active mTORC1 switches on anabolic pathways. Upon glucose starvation, the "inactive" v-ATPase and its partner Ragulator become accessible for AXIN binding, which in turn inhibits the GEF activity of Ragulator, leading to dissociation of mTORC1 from endosome. Starvation accumulates AMP to increase the affinity of AMPK for LKB1-bound AXIN; aberrantly high concentrations of AMPK could also stimulate AMPK activity directly through allosteric changes. As a result, glucose starvation leads to translocation of a significant portion of AXIN/LKB1 to the endosome, where AMPK is phosphorylated and activated by LKB1, switching on catabolic metabolism.
See also Figure S7.

and energy signals via a coordinated phosphorylation by AMPK and GSK3 to regulate cell growth. Cell *126*, 955–968.

Kalender, A., Selvaraj, A., Kim, S.Y., Gulati, P., Brûlé, S., Viollet, B., Kemp, B.E., Bardeesy, N., Dennis, P., Schlager, J.J., et al. (2010). Metformin, independent of AMPK, inhibits mTORC1 in a rag GTPase-dependent manner. Cell Metab. *11*, 390–401.

Kemp, B.E. (2004). Bateman domains and adenosine derivatives form a binding contract. J. Clin. Invest. *113*, 182–184.

Kim, E., Goraksha-Hicks, P., Li, L., Neufeld, T.P., and Guan, K.L. (2008). Regulation of TORC1 by Rag GTPases in nutrient response. Nat. Cell Biol. *10*, 935–945.

Laplante, M., and Sabatini, D.M. (2012). mTOR signaling in growth control and disease. Cell *149*, 274–293.

Li, Y., Xu, S.Q., Mihaylova, M.M., Zheng, B., Hou, X.Y., Jiang, B.B., Park, O., Luo, Z.J., Lefai, E., Shyy, J.Y.J., et al. (2011). AMPK phosphorylates and inhibits SREBP activity to attenuate hepatic steatosis and atherosclerosis in diet-induced insulin-resistant mice. Cell Metab. *13*, 376–388.

Ma, L., Chen, Z.B., Erdjument-Bromage, H., Tempst, P., and Pandolfi, P.P. (2005). Phosphorylation and functional inactivation of TSC2 by Erk implications for tuberous sclerosis and cancer pathogenesis. Cell *121*, 179–193.

Manning, B.D., Tee, A.R., Logsdon, M.N., Blenis, J., and Cantley, L.C. (2002). Identification of the tuberous sclerosis complex-2 tumor suppressor gene product tuberin as a target of the phosphoinositide 3-kinase/akt pathway. Mol. Cell *10*, 151–162.

Menon, S., Dibble, C.C., Talbott, G., Hoxhaj, G., Valvezan, A.J., Takahashi, H., Cantley, L.C., and Manning, B.D. (2014). Spatial control of the TSC complex integrates insulin and nutrient regulation of mTORC1 at the lysosome. Cell *156*, 771–785.

Moore, F., Weekes, J., and Hardie, D.G. (1991). Evidence that AMP triggers phosphorylation as well as direct allosteric activation of rat liver AMP-activated protein kinase. A sensitive mechanism to protect the cell against ATP depletion. Eur. J. Biochem. *199*, 691–697.

Murray, J.T., Panaretou, C., Stenmark, H., Miaczynska, M., and Backer, J.M. (2002). Role of Rab5 in the recruitment of hVps34/p150 to the early endosome. Traffic *3*, 416–427.

Nada, S., Hondo, A., Kasai, A., Koike, M., Saito, K., Uchiyama, Y., and Okada, M. (2009). The novel lipid raft adaptor p18 controls endosome dynamics by anchoring the MEK-ERK pathway to late endosomes. EMBO J. *28*, 477–489.

Oakhill, J.S., Chen, Z.P., Scott, J.W., Steel, R., Castelli, L.A., Ling, N., Macaulay, S.L., and Kemp, B.E. (2010). β-Subunit myristoylation is the gatekeeper for initiating metabolic stress sensing by AMP-activated protein kinase (AMPK). Proc. Natl. Acad. Sci. USA *107*, 19237–19241.

Oakhill, J.S., Steel, R., Chen, Z.P., Scott, J.W., Ling, N., Tam, S., and Kemp, B.E. (2011). AMPK is a direct adenylate charge-regulated protein kinase. Science *332*, 1433–1435.

Panchaud, N., Péli-Gulli, M.P., and De Virgilio, C. (2013). Amino acid deprivation inhibits TORC1 through a GTPase-activating protein complex for the Rag family GTPase Gtr1. Sci. Signal. *6*, ra42.

Potter, C.J., Pedraza, L.G., and Xu, T. (2002). Akt regulates growth by directly phosphorylating Tsc2. Nat. Cell Biol. *4*, 658–665.

Rink, J., Ghigo, E., Kalaidzidis, Y., and Zerial, M. (2005). Rab conversion as a mechanism of progression from early to late endosomes. Cell *122*, 735–749.

Roux, P.P., Ballif, B.A., Anjum, R., Gygi, S.P., and Blenis, J. (2004). Tumor-promoting phorbol esters and activated Ras inactivate the tuberous sclerosis tumor suppressor complex via p90 ribosomal S6 kinase. Proc. Natl. Acad. Sci. USA *101*, 13489–13494.

Rui, Y.N., Xu, Z., Lin, S.Y., Li, Q.X., Rui, H.L., Luo, W., Zhou, H.M., Cheung, P.Y., Wu, Z.G., Ye, Z.Y., et al. (2004). Axin stimulates p53 functions by activation of HIPK2 kinase through multimeric complex formation. EMBO J. *23*, 4583–4594.

Sakamoto, K., McCarthy, A., Smith, D., Green, K.A., Grahame Hardie, D., Ashworth, A., and Alessi, D.R. (2005). Deficiency of LKB1 in skeletal muscle prevents AMPK activation and glucose uptake during contraction. EMBO J. *24*, 1810–1820.

Sancak, Y., Peterson, T.R., Shaul, Y.D., Lindquist, R.A., Thoreen, C.C., Bar-Peled, L., and Sabatini, D.M. (2008). The Rag GTPases bind raptor and mediate amino acid signaling to mTORC1. Science *320*, 1496–1501.

Sancak, Y., Bar-Peled, L., Zoncu, R., Markhard, A.L., Nada, S., and Sabatini, D.M. (2010). Ragulator-Rag complex targets mTORC1 to the lysosomal surface and is necessary for its activation by amino acids. Cell *141*, 290–303.

Settembre, C., Fraldi, A., Medina, D.L., and Ballabio, A. (2013). Signals from the lysosome: a control centre for cellular clearance and energy metabolism. Nat. Rev. Mol. Cell Biol. *14*, 283–296.

Shackelford, D.B., and Shaw, R.J. (2009). The LKB1-AMPK pathway: metabolism and growth control in tumour suppression. Nat. Rev. Cancer *9*, 563–575.

Shaw, R.J., Kosmatka, M., Bardeesy, N., Hurley, R.L., Witters, L.A., DePinho, R.A., and Cantley, L.C. (2004). The tumor suppressor LKB1 kinase directly activates AMP-activated kinase and regulates apoptosis in response to energy stress. Proc. Natl. Acad. Sci. USA *101*, 3329–3335.

Shaw, R.J., Lamia, K.A., Vasquez, D., Koo, S.H., Bardeesy, N., Depinho, R.A., Montminy, M., and Cantley, L.C. (2005). The kinase LKB1 mediates glucose homeostasis in liver and therapeutic effects of metformin. Science *310*, 1642–1646.

Steinberg, G.R., and Kemp, B.E. (2009). AMPK in Health and Disease. Physiol. Rev. *89*, 1025–1078.

Steinberg, B.E., Huynh, K.K., Brodovitch, A., Jabs, S., Stauber, T., Jentsch, T.J., and Grinstein, S. (2010). A cation counterflux supports lysosomal acidification. J. Cell Biol. *189*, 1171–1186.

Stenmark, H., Parton, R.G., Steele-Mortimer, O., Lütcke, A., Gruenberg, J., and Zerial, M. (1994). Inhibition of rab5 GTPase activity stimulates membrane fusion in endocytosis. EMBO J. *13*, 1287–1296.

Woods, A., Johnstone, S.R., Dickerson, K., Leiper, F.C., Fryer, L.G.D., Neumann, D., Schlattner, U., Wallimann, T., Carlson, M., and Carling, D. (2003). LKB1 is the upstream kinase in the AMP-activated protein kinase cascade. Curr. Biol. *13*, 2004–2008.

Xiao, B., Heath, R., Saiu, P., Leiper, F.C., Leone, P., Jing, C., Walker, P.A., Haire, L., Eccleston, J.F., Davis, C.T., et al. (2007). Structural basis for AMP binding to mammalian AMP-activated protein kinase. Nature *449*, 496–500.

Zhang, Y.L., Guo, H.L., Zhang, C.S., Lin, S.Y., Yin, Z.Y., Peng, Y.Y., Luo, H., Shi, Y.Z., Lian, G.L., Zhang, C.X., et al. (2013). AMP as a low-energy charge signal autonomously initiates assembly of AXIN-AMPK-LKB1 complex for AMPK activation. Cell Metab. *18*, 546–555.

Zoncu, R., Bar-Peled, L., Efeyan, A., Wang, S., Sancak, Y., and Sabatini, D.M. (2011). mTORC1 senses lysosomal amino acids through an inside-out mechanism that requires the vacuolar H(+)-ATPase. Science *334*, 678–683.